

# Anomalous interactions in Higgs boson production at photon colliders

A. T. Banin, I. F. Ginzburg\*, I. P. Ivanov  
*Institute of Mathematics, Novosibirsk, Russia*  
 (November 24, 1998)

We discuss the potentialities of the non-standard interaction study via the Higgs boson production at photon ( $\gamma\gamma$  and  $e\gamma$ ) colliders. We estimate the scale of New Physics phenomena beyond the  $SM$  that can be seen in the experiments with Higgs boson production. In particular, the effect of new heavy particles within the  $SM$  is shown to be quite observable.

## I. INTRODUCTION

The discovery of the Higgs boson ( $H$ ) is the key problem of modern particle physics. A crucial point for the Standard Model ( $SM$ ), the Higgs boson remains elusive in the experiments being conducted currently. It is expected that the colliders of a new generation will have enough energy and large enough luminosity integral to discover a Higgs boson unambiguously. We assume that these efforts will be successful and discuss one of the subsequent series of problems.

Our point is: *The study of Higgs boson production at photon colliders ( $\gamma\gamma$  and  $e\gamma$ ) and in gluon fusion at hadron colliders (Tevatron and LHC) gives the best way to probe New Physics effects with a scale  $\Lambda > 1$  TeV at lower energies.*

At energies below  $\Lambda$  the above New Physics effects appear as some anomalous interactions of the particles already known (anomalies).

The Higgs boson interactions with photons ( $H\gamma\gamma$  and  $HZ\gamma$ ) or gluons ( $Hgg$ ) provide a radically new opportunity since the corresponding  $SM$  interactions arise only at the loop level. So the relative contribution of anomalies will be enhanced in these vertices. This is the leading idea that motivates us to study the processes

$$\gamma\gamma \rightarrow H, \quad \gamma\gamma \rightarrow HH, \quad e\gamma \rightarrow eH. \quad (1)$$

(The corresponding problems for the  $Hgg$  vertex extracted via the gluon fusion at Tevatron or LHC are studied elsewhere [1], [2].)

Usually, several effects of New Physics appear in the measurable cross sections simultaneously (for example, quadruple momentum and anomalous magnetic momentum of  $W$ , etc. in the reaction  $e^+e^- \rightarrow WW$ ). It is difficult to separate out a particular anomaly from the observed effects. Our second point is that *successive investigation of reactions (1) allows one to study different anomalies independently.*

The reaction  $\gamma\gamma \rightarrow H$  was originally studied in this regard in ref. [3] and the results were rederived in ref. [4]. The reaction  $e\gamma \rightarrow eH$  was analyzed in refs. [5], [6] for intermediate mass Higgs boson. (The same problems can be studied in the process  $e^+e^- \rightarrow H\gamma$ . However, the

cross section of this reaction is much lower, see, e.g., Ref. [7].)

In this paper we consider all reactions (1) from the common point of view. In Sec. II we discuss processes (1) in the Minimal Standard Model ( $MSM$ ). We present more accurate and detailed results than earlier treatment of the reaction  $e\gamma \rightarrow eH$  which is free from inaccuracies of previous papers (sometimes minor inaccuracies). In Sec. III we explore anomalies. First, we discuss the sense of observable anomalies. Next, we study effects from both the general anomalies and some specific scenarios of the New Physics – the  $SM$  with four generation of quarks and leptons or the  $SM$  with an additional heavy gauge boson. Finally, conclusions are drawn in Sec. IV.

## A. Preliminaries

Throughout the paper, we deal with the Higgs boson in the  $MSM$  with one Higgs doublet. We use modern parameters of the  $SM$  and assume  $M_H \gtrsim 90$  GeV [8]. We express results in terms of the Higgs field vacuum expectation value (VEV)  $v$ , which is related to the Fermi coupling constant  $G_F$ , and use abbreviations

$$v = (\sqrt{2}G_F)^{-1/2} = 246 \text{ GeV}, \\ c_W \equiv \cos\theta_W, \quad s_W \equiv \sin\theta_W.$$

In addition,  $\lambda_i$  are the helicities of photons and  $\zeta_e$  is the doubled electron helicity.

It is convenient to describe the  $H\gamma\gamma$  or  $HZ\gamma$  interaction via the Effective Lagrangians

$$\mathcal{L}_{H\gamma\gamma} = \frac{G_\gamma}{2v} F^{\mu\nu} F_{\mu\nu} H, \quad \mathcal{L}_{HZ\gamma} = \frac{G_Z}{v} F^{\mu\nu} Z_{\mu\nu} H; \quad (2) \\ G_i^{SM} = \frac{\alpha\Phi_i}{4\pi} \quad (i = \gamma \text{ or } Z).$$

Here  $F_{\mu\nu}$  and  $Z_{\mu\nu}$  are the standard field strength tensors. Factor  $v^{-1}$  is introduced to make the effective coupling constants  $G_i$  dimensionless. The last equation defines the specific normalization of these couplings within the  $SM$  (since they arise from triangle diagrams with charged fermions or  $W$  bosons circulating in loops, their natural scale is given by the fine structure constant  $\alpha$ ). The functions  $\Phi_i$  are written in Eqs. (8) – (11). The

corresponding partial decay widths of the Higgs boson are described via the quantities  $G_i$  by relations

$$\begin{aligned}\Gamma_{H \rightarrow \gamma\gamma} &= \frac{|G_\gamma|^2}{16\pi v^2} M_H^3, \\ \Gamma_{H \rightarrow Z\gamma} &= \frac{|G_Z|^2}{8\pi v^2} M_H^3 \left(1 - \frac{M_Z^2}{M_H^2}\right)^3.\end{aligned}\quad (3)$$

Since the  $\mathcal{SM}$  works well so far, we believe that the discussed anomalies give rise only to small corrections to the main the  $\mathcal{SM}$  couplings in our energy interval. So, in the analysis we assume that main Higgs boson decay rates as well as the total Higgs boson width remain practically the same as in the  $\mathcal{SM}$ .

Future linear colliders are intended to be complexes operating in both  $e^+e^-$  mode and **Photon Collider** ( $e\gamma$  and  $\gamma\gamma$ ) modes with the following typical parameters (that can be obtained without a specific optimization for the photon mode) [9,10] ( $E$  and  $\mathcal{L}_{ee}$  are the electron energy and luminosity of the basic  $e^+e^-$  collider).

- Characteristic photon energy  $E_\gamma \approx 0.8E$ .
- Annual luminosity  $\mathcal{L}_{\gamma\gamma} \approx 0.2\mathcal{L}_{ee}$ , typical  $\mathcal{L}_{\gamma\gamma} = 100 \text{ fb}^{-1}$ .
- Mean energy spread  $\langle \Delta E_\gamma \rangle \approx 0.07E_\gamma$ .
- Mean photon helicity  $\langle \lambda_\gamma \rangle \approx 0.95$  with variable sign [9].
- Circular polarization of photons can be transformed into the linear one [11].

(In other words, one can consider photon beams roughly monochromatic and arbitrary polarized.)

## II. THE PRODUCTION OF THE HIGGS BOSON IN THE $\mathcal{MSM}$

In this section we assume the ordinary variant of the  $\mathcal{MSM}$  with three fermion generations.

### A. Higgs boson production in $\gamma\gamma$ collisions

The most important process here is the **resonant Higgs boson production**  $\gamma\gamma \rightarrow H$ . Describing the luminosity distribution near its peak by the Lorentzian form, one obtains the cross section averaged over the luminosity distribution:

$$\langle \sigma \rangle \equiv \int \sigma(\sqrt{s}) \frac{1}{\mathcal{L}_{\gamma\gamma}} \frac{d\mathcal{L}_{\gamma\gamma}}{d\sqrt{s}} d\sqrt{s} = 8\pi(1 + \lambda_1\lambda_2) \frac{\Gamma_{H \rightarrow \gamma\gamma}}{M_H^3} \frac{M_H Br(H \rightarrow A)}{\Gamma_H + \Delta E_\gamma}.\quad (4)$$

Here  $Br(H \rightarrow A)$  is the branching ratio of the Higgs boson decay into a particular channel  $A$ .

Depending on the value of  $M_H$ , different final states should be used for the Higgs boson exploration ( $b\bar{b}$  for  $M_H < 140$  GeV,  $W^*W$  at  $120 \text{ GeV} < M_H < 190$  GeV,

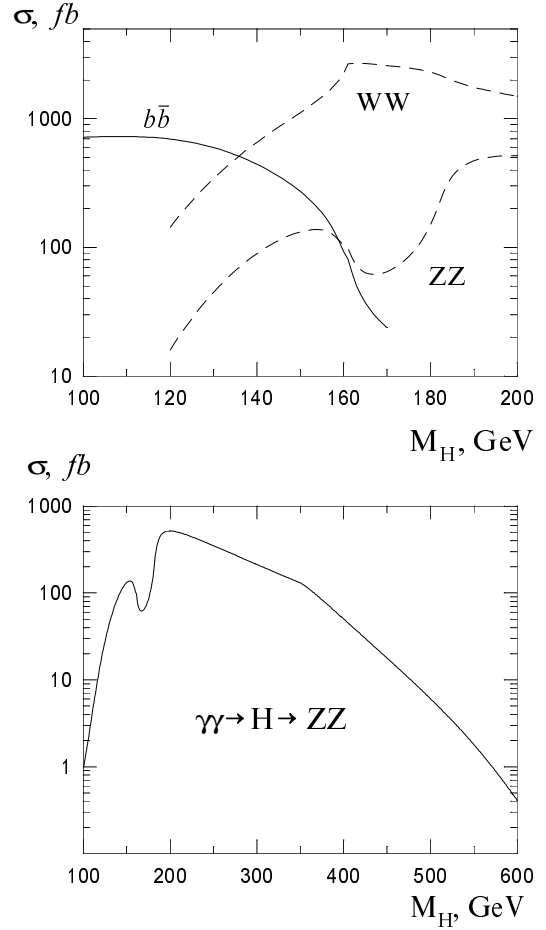


FIG. 1. The cross section of reaction  $\gamma\gamma \rightarrow H$  with some decay channels.  $\langle \lambda_1 \rangle = \langle \lambda_2 \rangle = 0.9$ ;  $20^\circ < \theta < 160^\circ$ .

$ZZ^*$  and  $ZZ$  at  $M_H > 140$  GeV, etc.). The cross sections of the Higgs boson production for the most important channels are plotted in Fig. 1. (For more detailed description see Refs. [12] – [15].)

Of special interest is the process  $\gamma\gamma \rightarrow HH$ . In ref. [16] the explicit calculation of this reaction was performed at one-loop level and a detailed analysis was carried out. At  $\sqrt{s} < 1$  TeV the total cross section of this reaction is less than 1 fb. This cross section exhibits a remarkable growth with both  $s$  and  $M_H$  increasing almost up to the kinematical limit, it is around a few fb for  $\sqrt{s} = 2$  TeV,  $M_H = 0.8$  TeV.

### B. $e\gamma \rightarrow eH$ process

We consider the experiments at c.m.s. energy squared  $s \gg M_H^2$  and with recording of a scattered electron having transverse momentum  $p_\perp \geq p_{\perp 0}$  which is related to the variable  $Q^2 \equiv -(p_e - p'_e)^2$  as

$$p_{\perp}^2 = Q^2 \left( 1 - \frac{M_H^2 + Q^2}{s} \right), \quad (5)$$

$$Q^2 \geq Q_{min}^2 = \frac{m_e^2 M_H^4}{s(s - M_H^2)}.$$

The cross section of this reaction is obviously less than (4). Therefore this process cannot be considered as a new source of Higgs bosons themselves. In addition to the new test of the  $SM$ , a novel feature of this process is the possibility to study  $HZ\gamma$  coupling. So, concerning this reaction, our main goal is to extract information about this interaction.

This process was studied in the frame of the Equivalent Photon Approximation in Refs. [17,18]. In this approach the  $HZ\gamma$  contribution is neglected. Recently this process has been considered in Ref. [5] for light Higgs boson ( $80 < M_H < 140$  GeV) with  $H \rightarrow b\bar{b}$  decay channel (and in Ref. [19] without a detailed analysis\*). It was shown that this process is helpful to study  $\gamma ZH$  interaction.

Here we consider this process in more detail and for a wider region of the Higgs boson masses. Accompanying all the calculations with qualitative discussion, we provide a clear-cut understanding of various properties of this and similar reactions.

**Different contributions and gauge invariance.** We deal with the amplitude of the physical process, that is, the projection of a calculated amplitude on mass shell states. We assume this procedure when decomposing an amplitude into several parts. (This projection does not affect the whole amplitude but it changes separate items.) It means that each considered item contains no contributions which are longitudinal in the momentum of external photon  $k$ .

This amplitude is decomposed into a sum of three items. The first one is the  $\gamma$  pole exchange contribution (photon exchange between scattered electron and triangle loop describing the  $\gamma^*\gamma \rightarrow H$  subprocess)  $\mathcal{A}_\gamma$ . This item is evidently *gauge invariant* since the longitudinal item in the photon propagator gives in the electron vertex  $q^\mu u(p') \gamma^\mu u(p) \rightarrow u(p')(\hat{p} - \hat{p}')u(p) = 0$ . The second item is the  $Z$  - pole exchange contribution  $\mathcal{A}_Z$  ( $Z$ -boson exchange between scattered electron and triangle loop describing the  $Z^*\gamma \rightarrow H$  subprocess.) This item is *approximately gauge invariant* with accuracy  $\sim m_e/M_Z$ . Indeed, the gauge dependent longitudinal item in the propagator gives in the electron vertex  $(q^\mu/M_Z)\bar{u}(p')\gamma^\mu(v + a\gamma^5)u(p) = (1/M_Z)\bar{u}(p')(\hat{p} - \hat{p}')(v + a\gamma^5)u(p) = 2a(m_e/M_Z)\bar{u}(p')\gamma^5 u(p)$ . The residual item is a sum of box diagrams themselves and relevant  $s$ - and  $u$ - pole diagrams, we denote it as box. [The box item can in turn be split into  $W$  and  $Z$  contributions (related to  $W$  and  $Z$  bosons circulating in loops.)

Having in mind a perturbative accuracy not better than  $\alpha \gg m_e/M_Z$ , we consider the above subdivision into 3 items gauge invariant<sup>†</sup>.

In these terms the cross section of reaction for the pure initial helicity states  $\lambda_\gamma = \pm 1$ ,  $\zeta_e = \pm 1$  can be written as

$$\frac{d\sigma}{dQ^2} = \frac{1}{64\pi s^2} \frac{\alpha^4 M_W^2 Q^2}{\sin^6 \theta_W} \times \left[ s^2(1 + \lambda_\gamma \zeta_e) |\mathcal{A}_\gamma + \mathcal{A}_Z + Z(s, u) + W(s, u)|^2 + u^2(1 - \lambda_\gamma \zeta_e) |\mathcal{A}_\gamma + \mathcal{A}_Z + Z(u, s) + W(u, s)|^2 \right], \quad (6)$$

$$(u = M_H^2 + Q^2 - s);$$

$$\mathcal{A}_\gamma = \frac{s_W^2}{Q^2 M_W^2} \Phi_\gamma, \quad \mathcal{A}_Z = \frac{s_W}{4c_W(Q^2 + M_Z^2)M_W^2} \Phi_Z. \quad (7)$$

The functions  $\Phi_i$  are split into the fermion and  $W$  boson parts which are written via the standard loop integrals

$$\Phi_\gamma = \sum_f N_c Q_f^2 \Phi^{1/2}(f) + \Phi_\gamma^1(W),$$

$$\Phi_Z = \sum_f N_c Q_f v_f \Phi^{1/2}(f) + \Phi_Z^1(W), \quad (8)$$

$$v_f = \frac{I_f - 2Q_f s_W^2}{2c_W s_W}.$$

Here

$$\Phi_\gamma^1(W) = \frac{[(3r_W + 2)C_{23}(r_W, w) - 8r_W C_0(w, r_W)]}{1 + w},$$

$$\Phi_Z^1(W) = \left( \frac{c_W}{s_W} - \frac{1}{4c_W s_W} \right) \Phi_\gamma^1(W) - \frac{(2 - r_W)C_{23}(w, r_W)}{4s_W c_W (1 + w)}; \quad (9)$$

$$\Phi^{1/2}(f) = -\frac{2r_f}{1 + w} [C_{23}(w, r_f) - C_0(w, r_f)].$$

$$\phi(r) = \begin{cases} -i \arcsin \frac{1}{\sqrt{r}} & \text{at } r > 1; \\ \ln \left( \frac{1 + \sqrt{1-r}}{\sqrt{|r|}} \right) - \frac{i\pi}{2} \theta(r) & \text{at } r < 1; \end{cases} \quad (10)$$

$$r_P = \frac{4M_P^2}{M_H^2}, \quad w = \frac{Q^2}{M_H^2};$$

$$C_0(w, r) = \phi^2(r) - \phi^2\left(-\frac{r}{w}\right),$$

$$C_{23}(w, r) = 1 + \frac{r}{1+w} C_0(w, r) + \frac{2w}{1+w} \left[ \sqrt{1-r} \phi(r) - \sqrt{1+\frac{r}{w}} \phi\left(-\frac{r}{w}\right) \right], \quad (11)$$

(here  $\sqrt{1-r} = i\sqrt{r-1}$  at  $r > 1$ ).

\* Note the obvious misprints in formulas (7),(8),(21) in Ref. [19].

<sup>†</sup> A similar subdivision without projection for the mass shell states is gauge dependent, see Ref. [7]; the gauge-dependent parts there disappear in the matrix element considered.

The mass shell values of  $\Phi_\gamma$  and  $\Phi_Z$  (at  $w = 0$ ) [20] are shown in Fig. 2. One can see that  $|\Phi_\gamma| \approx 5 \div 10$  for  $M_H < 350$  GeV and  $Re \Phi_\gamma$  changes its sign at  $M_H \approx 350$  GeV (due to a compensation between  $t$  quark and  $W$  boson loops). Typically  $\Phi_Z \approx 2\Phi_\gamma$ .

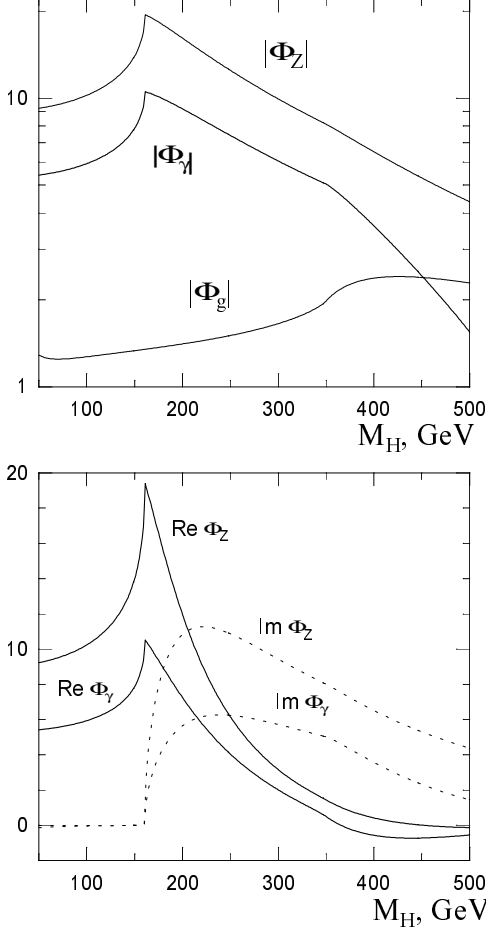


FIG. 2. Loop integrals for  $\gamma\gamma H$  and  $Z\gamma H$  interactions: absolute values and real and imaginary parts. The same loop integral for the  $ggH$  interaction is also shown for comparison.

**Qualitative analysis.** The total cross section of the process is estimated in the Equivalent Photon Approximation as  $(\alpha/\pi) \ln[s^2/(m_e^2 M_H^2)] \sigma_{\gamma\gamma \rightarrow H} \sim (10 \div 20)$  fb (see Fig. 3). The effect of  $HZ\gamma$  interaction is about several fb.

To understand the reaction better, we discuss the magnitude of separate contributions for different  $Q^2$  values. A typical box contribution is  $\propto 1/s$  whereas triangle effective couplings  $\Phi_i$  are  $s$  independent and depend on  $Q^2$  smoothly at  $Q^2 < M_H^2$ . So, at  $Q^2 \ll s$  both  $\mathcal{A}_\gamma$  and  $\mathcal{A}_Z$  contributions are enhanced due to small propagator denominators  $1/Q^2$  or  $1/(Q^2 + M_Z^2)$ . This enhancement is compensated partly by a (diffractive) factor  $\sim p_\perp$  from the  $e\bar{e}\gamma$  or  $e\bar{e}Z$  vertex. These items give the dominant contribution to the total cross section with the enhancement factor  $\sim \ln(M_H^2/Q_{min}^2)$  for

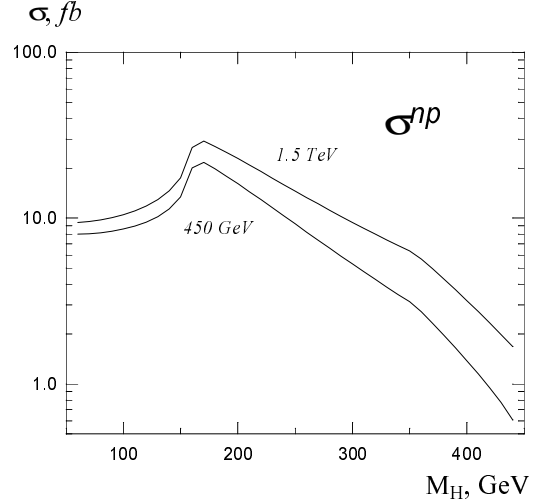


FIG. 3. Total unpolarized  $e\gamma \rightarrow eH$  cross section for  $\sqrt{s} = 450$  GeV and 1.5 TeV.

$|\mathcal{A}_\gamma|^2$  and  $\sim \ln(M_H^2/M_Z^2)$  for  $|2Re\mathcal{A}_\gamma^* \mathcal{A}_Z + \mathcal{A}_Z^2|$ . At  $Q^2 \ll M_Z^2$  and, consequently, in the total cross section photon contribution strongly dominates. With the growth of  $Q^2$  up to values comparable with  $M_Z^2$ , the contribution  $|2Re\mathcal{A}_\gamma^* \mathcal{A}_Z + \mathcal{A}_Z^2|$  becomes competitive with  $|\mathcal{A}_\gamma|^2$ . Finally, at  $Q^2 \sim s$  the box contribution becomes sizable too. Its relative contribution to the total cross section is less than  $Z$ -pole diagram by a factor  $\sim M_H^2/s$  with no large logarithms.

As we are interested in the extraction of the  $\gamma ZH$  interaction, we deduce from the above discussion that the  $Z$ -exchange contribution grows relatively in the cross section, integrated over the region  $p_\perp > p_{\perp 0}$  with large enough  $p_{\perp 0}$

$$\sigma(Q_0^2) = \int_{Q_0^2}^{s-M_H^2-Q_0^2} \frac{d\sigma(Q^2)}{dQ^2} dQ^2, \quad (12)$$

where quantity  $Q_0^2$  is related to  $p_{\perp 0}$  via eq. (5). The upper limitation here describes elimination of small transverse momenta of electrons scattered in a backwards direction.

The pole contributions in Eq. (12) are approximately independent on energy since the integral over  $Q^2$  is saturated at  $Q^2 \sim M_H^2$ , which is the scale of the decrease of the triangle loop itself with the growth of  $Q^2$ . Simultaneously, the box contribution decreases with  $s$  growth.

The second step in extracting the  $\gamma ZH$  vertex is to consider the cross sections  $d\sigma_L$  and  $d\sigma_R$  for the left hand and right hand polarized electrons. Neglecting box contributions these cross sections are expressed in terms of vector  $M_V$  and axial amplitudes  $M_A$ . The axial amplitude  $M_A$  utterly originates from the  $Z$  boson exchange ( $J^Z$ ), whereas the vector amplitude receives contributions from both the photon and  $Z$  boson:

$$M_V = \frac{1}{Q^2} J^\gamma + \frac{1-4\sin^2\theta_W}{Q^2+M_Z^2} J_V^Z, \quad (13)$$

$$M_A = \frac{1}{Q^2+M_Z^2} J_A^Z.$$

(Since  $1-4\sin^2\theta_W \ll 1$ ,  $M_V \propto J^\gamma$  with good accuracy.)

With this notation,  $d\sigma_{L,R} \propto |M_V \pm M_A|^2$ . The difference between the cross sections  $\Delta\sigma = \sigma_L - \sigma_R$  and the cross section for the unpolarized electrons  $\sigma^{np}$  is

$$\Delta d\sigma \equiv d\sigma_L - d\sigma_R \propto \text{Re}(M_V^* M_A), \quad (14)$$

$$d\sigma^{np} \equiv \frac{d\sigma_L + d\sigma_R}{2} \propto (|M_V|^2 + |M_A|^2).$$

In other words, the quantity  $\Delta\sigma$  directly reveals the magnitude of  $\gamma Z^* H$  interaction.

To see the role of the initial photon helicity in this process, it is instructive to recall that a longitudinally polarized electron transmits a part  $x \approx M_H^2/s$  of its polarization to an exchanged photon [21]. The same estimate is also valid for an exchanged  $Z$ -boson. On the other hand, a Higgs boson can be produced only in the total spin zero state. Therefore, variation of the photon helicity changes the rate of the Higgs boson production in  $e\gamma$  collisions. This influence decreases with  $s/M_H^2$  growth.

**Main radiative corrections.** We start our calculations from the value  $\alpha(0) = 1/137$  which is the fine structure constant for the real photon independent from its energy. The identical electric charge in all electromagnetic vertices is necessary to have gauge invariant QED and in other vertices to have gauge invariant EW theory.

There are three types of radiative corrections for the process discussed.

(1) Corrections related to the photon emission, etc., from virtual heavy particles are  $\sim \alpha$  and can be omitted at our 1 % level of accuracy. The QCD radiative corrections (for the quark loops) also become small enough after suitable renormalization of quark masses [22].

(2) There are large (logarithmic) radiative corrections connected with light particle ( $e^+e^-$ ,  $\mu^+\mu^-$ , etc.) loops in the propagators of the photon or  $Z$  and similar  $e\nu$ , etc., loops in the  $W$  propagator. Their effect could be accounted for by the change  $\alpha(0) \rightarrow \alpha(Q^2)$ . Since the characteristic value of  $Q^2$  is  $\sim M_Z^2$  in our case, we change  $\alpha(0) = 1/137$  to  $\alpha(M_Z^2) = 1/128$  in two vertices of diagrams where neither real photon nor Higgs boson is involved.

(3) There are an initial and final state radiation (ISR and FSR) of electron. The ISR reduce the initial electron energy as compared with our calculations. In addition, the observed result is smoothed over some interval of  $Q^2$  since the visible transverse momentum of electron  $p_{\perp,vis}$  differs from the "true" one due to the emission of a photon mainly in FSR. Fortunately, the cross sections  $\sigma(Q_0^2)$  (12) depend only slightly<sup>‡</sup> on  $s$ . The effect of the differ-

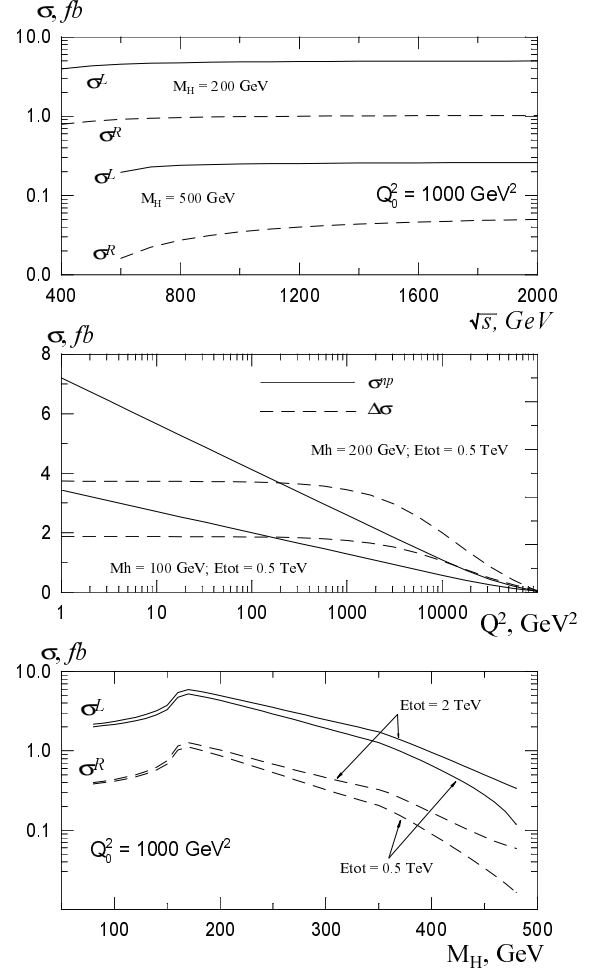


FIG. 4. The  $e\gamma \rightarrow eH$  cross section:  $s$ -dependence of  $\sigma_L$  and  $\sigma_R$  (upper),  $Q^2$ -dependence of  $\sigma^{np}$  and  $\Delta\sigma$  (middle) and  $M_H$ -dependence for  $\sigma_L$  and  $\sigma_R$  (lower).

ence between true  $p_{\perp}$  and  $p_{\perp,vis}$  depends on the method of recording the scattered electron, it can be considered in a more detailed simulation. For example, this effect is small at the calorimetric method of electron momentum recording. These effects are considered in the standard simulation.

### Numeral results.

For our calculations of the box contribution we transform corrected formulas from Ref. [7] (obtained for the  $e^+e^- \rightarrow H\gamma$  process) to our kinematical region. [Note that the fermion contribution in formulas (12), (13) of that paper should be twice larger.] These equations are rather complicated and the box contribution to the cross section is rather small. We gave all relevant formulas

<sup>‡</sup> This is in contrast to the total cross section, it depends on  $s$  mainly via the contribution of a very small  $Q^2$  near  $Q_{min}^2$  (5).

| $\sqrt{s} = 1.5 \text{ TeV} \quad Q^2 = 1000 \text{ GeV}^2$   |                          |                            |                     |                   |               |
|---|--------------------------|----------------------------|---------------------|-------------------|---------------|
| $M_H = 100 \text{ GeV}$   |                          |                            |                     |                   |               |
| $\zeta_e, \lambda_\gamma$   | $ \gamma\gamma H ^2, fb$ | $\gamma Z\text{-int.}, fb$ | $ \gamma ZH ^2, fb$ | pole-box int., fb | $ box ^2, fb$ |
| -1; -1  | 0.929                    | 0.852                      | 0.273               | -0.0160           | 0.0105        |
| -1; +1  | 0.903                    | 0.811                      | 0.253               | 0.0363            | 0.0034        |
| +1; -1  | 0.903                    | -0.700                     | 0.188               | 1.3e-6            | 1.2e-5        |
| +1; +1  | 0.929                    | -0.735                     | 0.203               | -2.5e-4           | 2.5e-4        |
| $\sigma_L = 2.03 \text{ fb}, \sigma_R = 0.39 \text{ fb}, \sigma^{np} = 1.21 \text{ fb}, \Delta\sigma = 1.64 \text{ fb}$ |                          |                            |                     |                   |               |
| $M_H = 200 \text{ GeV}$   |                          |                            |                     |                   |               |
| $\zeta_e, \lambda_\gamma$   | $ \gamma\gamma H ^2, fb$ | $\gamma Z\text{-int.}, fb$ | $ \gamma ZH ^2, fb$ | pole-box int., fb | $ box ^2, fb$ |
| -1; -1  | 2.06                     | 1.77                       | 0.537               | 0.0200            | 0.0234        |
| -1; +1  | 1.96                     | 1.65                       | 0.490               | 0.0702            | 0.0038        |
| +1; -1  | 1.96                     | -1.43                      | 0.364               | -7.0e-5           | 1.4e-5        |
| +1; +1  | 2.06                     | -1.53                      | 0.399               | -5.2e-4           | 5.0e-4        |
| $\sigma_L = 4.29 \text{ fb}, \sigma_R = 0.91 \text{ fb}, \sigma^{np} = 2.60 \text{ fb}, \Delta\sigma = 3.38 \text{ fb}$ |                          |                            |                     |                   |               |
| $M_H = 500 \text{ GeV}$   |                          |                            |                     |                   |               |
| $\zeta_e, \lambda_\gamma$   | $ \gamma\gamma H ^2, fb$ | $\gamma Z\text{-int.}, fb$ | $ \gamma ZH ^2, fb$ | pole-box int., fb | $ box ^2, fb$ |
| -1; -1  | 0.059                    | 0.083                      | 0.085               | 0.0056            | 0.0144        |
| -1; +1  | 0.045                    | 0.066                      | 0.061               | 0.0163            | 0.0032        |
| +1; -1  | 0.045                    | -0.057                     | 0.045               | -5.9e-5           | 4.8e-6        |
| +1; +1  | 0.059                    | -0.072                     | 0.063               | -0.0013           | 1.5e-4        |
| $\sigma_L = 0.22 \text{ fb}, \sigma_R = 0.05 \text{ fb}, \sigma^{np} = 0.13 \text{ fb}, \Delta\sigma = 0.17 \text{ fb}$ |                          |                            |                     |                   |               |

TABLE I. Different contributions into the cross section of  $e\gamma \rightarrow eH$  process for various polarization states.

| $\sqrt{s} = 1.5 \text{ TeV}$ |                         |                    |                         |                    |                         |                    |
|------------------------------|-------------------------|--------------------|-------------------------|--------------------|-------------------------|--------------------|
| $Q^2,$<br>GeV <sup>2</sup>   | $M_H = 100 \text{ GeV}$ |                    | $M_H = 200 \text{ GeV}$ |                    | $M_H = 500 \text{ GeV}$ |                    |
|                              | $\sigma_{np}, fb$       | $\Delta\sigma, fb$ | $\sigma_{np}, fb$       | $\Delta\sigma, fb$ | $\sigma_{np}, fb$       | $\Delta\sigma, fb$ |
| 1                            | 3.23                    | 1.75               | 7.42                    | 3.65               | 0.26                    | 0.19               |
| 3                            | 2.90                    | 1.75               | 6.65                    | 3.65               | 0.24                    | 0.19               |
| 10                           | 2.56                    | 1.75               | 5.81                    | 3.65               | 0.21                    | 0.19               |
| 30                           | 2.23                    | 1.75               | 5.04                    | 3.64               | 0.19                    | 0.19               |
| 100                          | 1.88                    | 1.74               | 4.20                    | 3.62               | 0.17                    | 0.19               |
| 300                          | 1.56                    | 1.71               | 3.44                    | 3.57               | 0.15                    | 0.19               |
| 1000                         | 1.21                    | 1.63               | 2.61                    | 3.38               | 0.13                    | 0.18               |
| 3000                         | 0.89                    | 1.44               | 1.86                    | 2.94               | 0.11                    | 0.16               |
| 10000                        | 0.55                    | 1.02               | 1.08                    | 1.98               | 0.08                    | 0.11               |
| 30000                        | 0.27                    | 0.53               | 0.49                    | 0.96               | 0.05                    | 0.06               |

TABLE II.  $Q^2$  dependence of  $\Delta\sigma$  and  $\sigma_{np}$ .

in the Appendix. We performed several checks to verify these expressions. First, we numerically checked the consistency of analytical formulas for scalar loop integrals. For this purpose we compared numbers obtained from our formulas and those obtained with the FF package [23]. We found that at a typical phase space point the two approaches give coincident results for all loop integrals up to nine significant digits or better. In addition, we examined the behavior near the points  $Q^2, u = 0$  of the box contribution decomposed into several scalar loops terms. The used forms of loop integrals are singular in this point. However, this singularity is absent in the amplitude. Indeed, near these points we observed eight digit cancellation among these terms until  $Q^2, |u| \sim 0.01 \text{ GeV}^2$ . (At lower values of  $Q^2, |u|$  both our formulas and the FF package yield numerically unstable results due to computer precision limitations.) Second, comparing different contributions separately, we found complete agreement with the results of Ref. [5] after removal of minor

inaccuracies there<sup>§</sup>.

These exact calculations confirm the above qualitative analysis. Some numerical data with different contributions can be found in Table I.

A detailed analysis of the numbers obtained shows that the pole contributions in  $\sigma(Q^2)$  become practically independent on  $s$  already at the moderate energy, whereas the box contribution and the cross section difference for opposite initial photon helicities decreases with  $s$  growth. With the growth of  $Q_0^2$ , the photon contribution is reduced whereas the  $Z$  contribution has only a weak dependence on  $Q_0$  unless  $Q_0^2 \gtrsim M_Z^2$ . This behavior is clearly seen in Table II, where  $\sigma^{np}$  and  $\Delta\sigma$  are given for various  $Q^2$  cut off. Last, the box items contribute less than 0.1 fb to the total cross section at the considered energies. These results are summarized in Fig. 4, where various dependencies for the cross sections are presented.

*The conclusions:*

- The  $e\gamma \rightarrow eH$  process is observable for a wide enough interval of Higgs boson masses and with large enough  $Q_0^2$  for different polarizations of colliding particles.
- The  $\gamma - Z$  exchange interference is strongly enhanced for the polarized cross sections. The effect of the  $\gamma ZH$  interaction becomes relatively large at  $p_\perp > 10$  GeV.
- The contribution of  $Z$ -pole exchange is saturated at  $p_{\perp 0} \approx 30$  GeV. It decreases slowly with  $Q_0^2$  growth up to  $M_Z^2$ . The values of  $\sigma_{L,R}(Q^2)$  at  $Q_0^2 \geq 1000$  GeV<sup>2</sup> depend weakly on  $s$ .
- The measurements of polarized cross sections at  $p_\perp > p_{\perp,0}$  with  $p_{\perp,0} = (10 \div 50)$  GeV provide an opportunity to extract complete information about the  $HZ\gamma$  vertex without reduction of *useful* statistics.
- If  $M_H < 300$  GeV, the cross sections increases slowly with the growth of c. m. energy above 500 GeV. From this it follows that the initial photon energy spread affects the result weakly.

### III. HIGGS BOSON ANOMALOUS INTERACTION

#### A. The Effective Lagrangian

Assuming that at very small distances some New Physics comes into play, one can consider the  $\mathcal{SM}$  as the low energy limit of this yet unknown theory with a characteristic scale of new phenomena  $\Lambda > 1$  TeV. At energies below  $\Lambda$  this underlying theory manifests itself as

some anomalous interactions (*anomalies*) of known particles. These interactions can be described by an Effective Lagrangian which is written as an expansion in  $\Lambda^{-1}$  starting from the  $L_{SM}$  — Lagrangian of the  $\mathcal{SM}$

$$L_{eff} = L_{SM} + \sum_{k=1}^{\infty} \Delta L_k, \quad (15)$$

$$L_{SM} = -\frac{B_{\mu\nu}B^{\mu\nu}}{4} - \frac{W_{\mu\nu}^i W^{i\mu\nu}}{4}, \quad \Delta L_k = \sum_r \frac{d_{rk} \mathcal{O}_{rk}}{\Lambda^k}.$$

Here the dimension of operators  $\mathcal{O}_{rk}$  is  $4+k$ ,  $B_{\mu\nu}$ ,  $W_{\mu\nu}^i$  are the standard field strength tensors, and the covariant derivative for a weak isospin Higgs doublet is  $D_\mu = \partial_\mu + ig'B_\mu/2 + ig\tau^i W_\mu^i/2$ .

It is usually assumed that the symmetry of  $L_{eff}$  is the same as that of  $L_{SM}$ . For this case  $\Delta L_1 = 0$ . We consider the next largest term  $\Delta L_2$ . The whole set of dimension six operators that can appear in  $\Delta L_2$  is given in refs. [24]- [26]. Only five of them give rise to anomalous  $H\gamma\gamma$  or  $HZ\gamma$  interactions [26]:

$$\begin{aligned} \mathcal{O}_{BB} &= \phi^+ B_{\mu\nu} B^{\mu\nu} \phi; & \mathcal{O}_{WW} &= \phi^+ W_{\mu\nu}^i W^{i\mu\nu} \phi; \\ \mathcal{O}_{BW} &= \phi^+ B_{\mu\nu} \tau^i W^{i\mu\nu} \phi; \\ \mathcal{O}_B &= i(D_\mu \phi)^+ B^{\mu\nu} (D_\nu \phi); \\ \mathcal{O}_W &= i(D_\mu \phi)^+ \tau^i W^{i\mu\nu} (D_\nu \phi). \end{aligned} \quad (16)$$

The standard transformation of the  $\mathcal{SM}$  conserves only the neutral component of the doublet:  $\phi \Rightarrow [0, (v + H)/\sqrt{2}]$ . In other words,  $(\phi^+ \phi) \Rightarrow (H^2 + 2Hv + v^2)/2$ ,  $(\phi^+ \tau^i \phi) \Rightarrow -(H^2 + 2Hv + v^2)\delta_{i3}/2$ . The part of  $\Delta L_2$  resulting from operators (16) after this replacement is decomposed for two items.

The item of interest describes nonstandard interactions of a Higgs boson with gauge bosons. Going from fields  $W^3$  and  $B$  to the physical fields  $A$  and  $Z$ , one immediately reveals that anomalous  $\gamma\gamma H$  and  $\gamma ZH$  interactions arising from all five operators are of *the same pattern*. All these contributions can be summarized in the expression

$$\Delta L_v = (2Hv + H^2) \left( \theta_\gamma \frac{F_{\mu\nu} F^{\mu\nu}}{2\Lambda_\gamma^2} + \theta_Z \frac{Z_{\mu\nu} F^{\mu\nu}}{\Lambda_Z^2} \right) \quad (17)$$

$$(\theta_i = \pm 1).$$

Here we introduced  $\Lambda_i$  by

$$\begin{aligned} \frac{\theta_\gamma}{\Lambda_\gamma^2} &= \frac{1}{\Lambda^2} (s_W^2 d_{WW} + c_W^2 d_{BB} - c_W s_W d_{WB}), \\ \frac{\theta_Z}{\Lambda_Z^2} &= \frac{1}{2\Lambda^2} [\sin 2\theta_W (d_{WW} - d_{BB}) \\ &\quad \cos 2\theta_W d_{WB} + \frac{\bar{q}}{4} (d_W - d_B)]. \end{aligned} \quad (18)$$

(Sometimes we write the product  $\theta_i \Lambda_i$  instead of  $\Lambda_i$  and  $\theta_i$  separately.)

In the detailed treatment of our processes the effective couplings in eq. (2) are sums of the  $\mathcal{SM}$  contributions and anomalies:

<sup>§</sup> We are grateful V. Ilyin for the detail discussion of this point.

$$G_i = G_i^{SM} + \Delta G_i \equiv \frac{\alpha}{4\pi}(\Phi_i + \Delta\Phi_i)$$

$$G_\gamma = \frac{\alpha}{4\pi}\Phi_\gamma + \frac{\theta_\gamma v^2}{\Lambda_\gamma^2}, \quad G_Z = \frac{\alpha}{4\pi}\Phi_Z + \frac{\theta_Z v^2}{\Lambda_Z^2}. \quad (19)$$

The residual items of  $L_{eff}$  describe anomalous  $HWW$  and  $HZZ$  interactions or contain no Higgs field operators. The extraction of these anomalies (from other experiments) is a more difficult task since they appear in interactions where the  $SM$  couplings occur at the tree level. The item without Higgs field is

$$\frac{v^2}{2\Lambda^2} (d_{BB}B_{\mu\nu}B^{\mu\nu} + d_{WW}W_{\mu\nu}^iW^{i\mu\nu} - d_{BW}B_{\mu\nu}W^{3\mu\nu}).$$

The first two terms here are absorbed in  $L_{SM}$  after renormalization  $W^{i\mu} \rightarrow W^{i\mu}(1 - 2d_{WW}v^2/\Lambda^2)^{1/2}$ ;  $B^\mu \rightarrow B^\mu(1 - 2d_{BB}v^2/\Lambda^2)^{1/2}$ . They give no observable effects. The  $d_{BW}$  term introduces an additional  $B - W^3$  mixing and thus changes the value of the Weinberg angle. It is constrained by the data [26].

Eq. (17) is the final form that can be used for the discussion of the considered experiments. The separate information about different parameters  $d_{rk}$  can be obtained only if one has additional information about their inter-relation (either in some separate theory or using additional experimental data). One should note in this respect that the subdivision of  $HZ\gamma$  anomaly for two items [27] gives no observable effects.

The relation between our quantities  $\Lambda_i$  ( $i = \gamma$  or  $Z$ ) and the mass scale of New Physics is a delicate question. Indeed, our anomalies can originate only from loops with circulating new heavy particles. Each loop contribution contains factor  $1/(4\pi)^2$ , and it seems reasonable to add this factor in the relation between our  $\Lambda_i$  and the scale of New Physics [28]. Moreover, the coupling with photons seem responsible for a stronger limitation. Indeed, the interaction with charged particles is determined by its electric charge. Therefore,  $d_a$  is additionally  $\propto \alpha$ .

In fact, the picture is more interesting. Let, for example, the New Physics contain some fermion with mass  $M_f \gg M_H$  and electric charge  $Q_f e$  which interaction with Higgs field is of Yukawa type but the coupling constant  $g_f$  is independent on  $M_f$  (another mechanism of mass generation is realized). In accordance with Eqs. (8), (21), the corresponding loop adds an anomaly contribution with

$$\Delta G = -\frac{4}{3}\alpha Q_f^2 \frac{g_f}{4\pi M_f}$$

$$\Rightarrow M_f = Q_f^2 \frac{g_f}{4\pi} \left( \frac{0.2\Lambda_\gamma}{1 \text{ TeV}} \right)^2 \text{ TeV} \quad (\theta_\gamma = -1). \quad (20)$$

In this respect, for example, the value  $\Lambda_\gamma = 30 \text{ TeV}$  which can be obtained from the data, corresponds to  $M_f = 35(g/4\pi)Q_f^2 \text{ TeV} = 2.8gQ_f^2 \text{ TeV}$  for each new charged fermion.

One should note that the perturbative theory series for Yukawa coupling is expanded in terms of the parameter  $(g_f/4\pi)^2$ . Therefore, our estimate remains valid until  $(g_f/4\pi)^2 \lesssim 1$  giving high enough  $M_f$ .

Moreover, the idea about factor  $\alpha$  is not completely precise. For example, the above new fermion can be a point like Dirac monopole (with  $\alpha \rightarrow 4/\alpha$ )!?

In principle, the anomaly  $H^2 F_{\mu\nu} F^{\mu\nu}$  can appear from items that do not contain parts linear in the Higgs field. But these new items originate from operators of eighth order in  $L_{eff}$ . Therefore, their natural magnitude is  $(v/\Lambda)^4$  and we neglect them.

Possible  $\mathcal{CP}$  violating terms in the anomalous interactions constitute a special problem. This will be discussed separately.

## B. Simplest variant of New Physics — new heavy particles within $\mathcal{MSM}$

The simplest variant of New Physics is the "trivial" extension of  $\mathcal{MSM}$  with the addition of new heavy generations of quarks and leptons  $f'$  (modern data does not forbid existence of such extra generations having heavy neutrinos with mass  $m_\nu > 45 \text{ GeV}$ ) or some additional heavy  $W'$  bosons. In the  $\mathcal{MSM}$  the Yukawa coupling constants of these new particles with the Higgs boson are proportional to their masses  $M_i$ . Therefore, there is no decoupling in the interactions of the Higgs boson induced by these new particles in intermediate states. In particular, the loops for the  $H\gamma\gamma$ ,  $HZ\gamma$ , and  $Hgg$  interactions are left finite at  $M_i^2 \gg M_H^2, Q^2$  [20]. (The Yukawa interaction of these quarks with the Higgs boson become strong if their masses are larger than  $4\pi v \approx 3 \text{ TeV}$ .)

The corresponding new items in an Effective Lagrangian are calculated easily with the aid of eqs. (8)–(11) for both variants of new heavy gauge charged vector boson ( $W'$ ) or one extra generation of heavy quarks and leptons ( $f'$ ):

$$\Delta\Phi_\gamma(W') = 7, \quad \Delta\Phi_Z(W') = \frac{31 - 42s_W^2}{6s_W c_W} \approx 8.41; \quad (21)$$

$$\Delta\Phi_\gamma(f') = -32/9, \quad \Delta\Phi_Z(f') = \frac{32s_W^2 - 12}{9s_W c_W} \approx -1.21.$$

In terms of Effective Lagrangian (17) and Eq. (19) these quantities correspond to

$$\theta_\gamma \Lambda_\gamma(W') = 5.4 \text{ TeV}, \quad \theta_Z \Lambda_Z(W') = 4.9 \text{ TeV};$$

$$\theta_\gamma \Lambda_\gamma(f') = -7.6 \text{ TeV}, \quad \theta_Z \Lambda_Z(f') = -13 \text{ TeV}. \quad (22)$$

Note that the entire fermion generation contribution in  $\Delta\Phi$  is twice as large as the  $t'$ -quark contribution.

These quantities are so large (compare them with Fig. 2) that they change dramatically  $\gamma\gamma H$  and  $\gamma Z H$  couplings (as well as  $ggH$  coupling). This leads to strong departures in corresponding decay widths and production cross sections. Therefore, the effect of new heavy particles in the  $SM$  is easily observable in all channels discussed.



Let us discuss corresponding variations in the processes considered in more detail.

### Photon collisions, $\gamma\gamma \rightarrow H$

New vector boson causes a dramatic enhancement of the cross section throughout the whole range of the Higgs boson mass (by a factor  $3 \div 100$ ) (see Fig. 5).

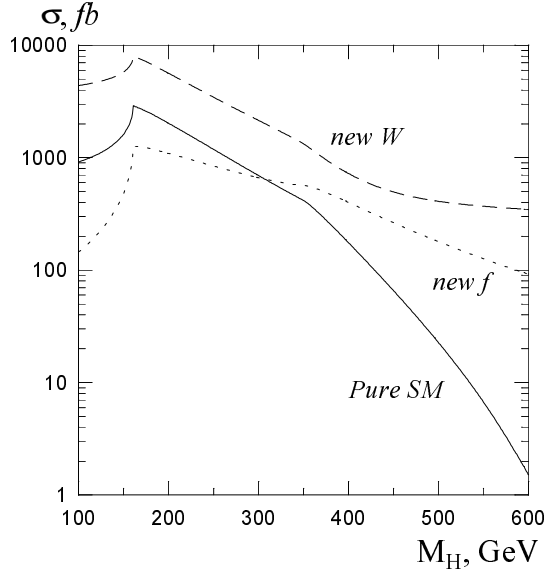


FIG. 5. The effect of new particles within the SM on  $\gamma\gamma \rightarrow H$  cross section.  $\langle \lambda_1 \rangle = \langle \lambda_2 \rangle = 0.9$ ;  $20^\circ < \theta < 160^\circ$ .

The fourth fermion generation causes a destructive effect for  $M_H < 300$  GeV, but also enlarges the rate of the Higgs boson production for higher values of  $M_H$ . This generation changes the cross section by a factor  $0.2 \div 50$  depending on the Higgs boson mass.

### Photon collisions, $\gamma\gamma \rightarrow HH$ .

In the considered case of a heavy new particles  $M_i \gg M_H$  and at  $M_i^2 \gg s$ , additional items to the amplitudes calculated in Ref. [16] are written in the form of the  $\gamma\gamma HH$  item in Eq. (17) with coupling constant (21). Therefore, the considered anomalous Higgs boson production in the  $\gamma\gamma \rightarrow H$  reaction should be accompanied by a deviation of the  $HH$  production rate in the process  $\gamma\gamma \rightarrow HH$ . A similar opportunity was studied first in [3].

Neglecting the small SM contribution, one has two diagrams for this reaction from interaction (17), the point-like one and  $\gamma\gamma \rightarrow H \rightarrow HH$ . Provided that the  $HHH$  vertex is the same as in the  $\mathcal{MSM}$ , the resulting cross section is

$$\begin{aligned} \sigma_{\gamma\gamma \rightarrow HH} &= (1 + \lambda_1 \lambda_2) \frac{s}{16\pi\Lambda_\gamma^4} \left( \frac{s + 2M_H^2}{s - M_H^2} \right)^2 \sqrt{1 - \frac{4M_H^2}{s}} \\ &\approx 7.7(1 + \lambda_1 \lambda_2) \frac{s(\text{TeV}^2)}{\Lambda_\gamma^4} \text{ pb.} \end{aligned} \quad (23)$$

The last approximation is valid just above the threshold. The angular distribution of produced  $H$  is roughly isotropic.

In particular, the existence of new heavy  $W'$  or fourth generation in the SM gives the cross sections

$$\begin{aligned} \sigma_{\gamma\gamma \rightarrow HH}(W') &\approx 73 \text{ fb} \times s(\text{TeV}^2), \\ \sigma_{\gamma\gamma \rightarrow HH}(f') &\approx 19 \text{ fb} \times s(\text{TeV}^2). \end{aligned} \quad (24)$$

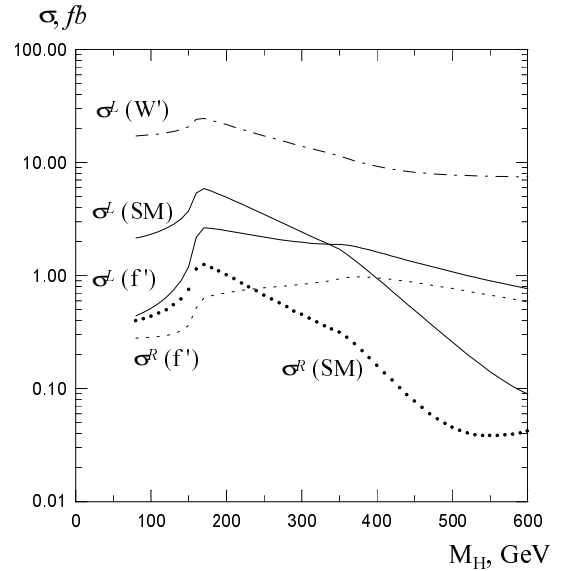


FIG. 6. The effect of new particles within the SM on  $e\gamma \rightarrow eH$  cross section.  $\sqrt{s} = 1.5 \text{ TeV}$ ,  $Q^2 = 1000 \text{ GeV}^2$ .

### Electron-photon collisions, $e\gamma \rightarrow eH$ .

Figure 6 represents the effect of new heavy particles on  $e\gamma \rightarrow eH$  cross sections. It is seen that the effect of the modified  $HZ\gamma$  coupling is extremely large for a heavy gauge vector boson and it is large for new heavy particles from the fourth generation.

*The Higgs boson production at Tevatron and LHC.* The main mechanism of the Higgs boson production at hadron colliders is gluon fusion. The Higgs boson coupling with gluons arises from triangle diagrams with circulating quarks. It is described by the quantity  $\Phi_g \propto \sum_q \Phi^{1/2}(r_q)$ . The major contribution is given by a  $t$  quark loop. An additional new gauge boson  $W'$  does not influence this effective coupling while adding of a new fermion generation would increase this coupling by a factor of about 3. This results in a tremendous growth of the Higgs

boson production cross section by a factor  $9 \div 6$  (depending on  $M_H$ ). This effect may be seen in the forthcoming experiments at the upgraded Tevatron by looking for an excess of  $\tau^+\tau^-$  events for  $100 < M_H < 140$  GeV and it will be clearly observed in all decay channels at LHC [1].

In some particular channel similar effects also might have another origin. However, this "miraculous" imitation seem hardly probable in the whole set of production channels just discussed. For instance, the modification of  $H\gamma\gamma$ ,  $HZ\gamma$ , or  $Hgg$  effective couplings caused by fourth generation can be mimicked in each channel in the two Higgs doublet model with some relations among parameters of the model ( $\beta$  and  $\alpha$ ). However, it happens at different values of  $\beta$  and  $\alpha$  for different couplings and overall imitation of all loop obliged couplings is impossible in this model [29].

### C. General anomalies

Let us consider the case when the effects of New Physics have another nature, e. g., SUSY, Technicolour, etc., but there are no new heavy particles within the  $SM$  sector. In this case, the scale of new effects is given by parametrization (17). These effects for the processes  $\gamma\gamma \rightarrow H$  and  $\gamma\gamma \rightarrow HH$  were considered first in ref. [3]. A more detailed treatment of process  $\gamma\gamma \rightarrow H$ , counting the interference with  $SM$  quantities was performed in Ref. [4] in the relatively narrow region of  $M_H$  and with an unrealistic luminosity distribution. These anomalies for the process  $e\gamma \rightarrow eH$  were considered in ref. [6] for  $M_H \leq 140$  GeV.

As we have seen, new particles within the  $SM$  resulted in large effects on  $\gamma\gamma \rightarrow H$  and  $e\gamma \rightarrow eH$  cross sections. These effects correspond to large enough scales (22). Therefore, the *ultimate* values of  $\Lambda_i$  that can be experimentally analyzed are higher.

Let us note that the sensitivity of process  $\gamma\gamma \rightarrow H$  to the  $\Lambda_\gamma$  is much higher than that of process  $e\gamma \rightarrow eH$ . Indeed, the observed cross section in the latter case is lower than that in the  $\gamma\gamma$  collision. The same physical background is unavoidably transferred to the  $e\gamma$  case (with corresponding reduction of effective luminosity). For example, background  $\gamma\gamma \rightarrow b\bar{b}$  turns into  $e\gamma \rightarrow e\bar{b}\bar{b}$  with the two photon mechanism of  $b\bar{b}$  pair production. In addition, additional backgrounds could arise in  $e\gamma$  collisions, such as  $e\gamma \rightarrow e\bar{b}\bar{b}$  with one photon (bremsstrahlung) mechanism of  $b\bar{b}$  pair production.

Therefore, *the process  $\gamma\gamma \rightarrow H$  should be used for the derivation of  $\Lambda_\gamma$ , and then  $\Lambda_Z$  should be extracted from the process  $e\gamma \rightarrow eH$  provided  $\Lambda_\gamma$  is known.* Thus, we separate these effects and discuss the  $HZ\gamma$  anomaly in the reaction  $e\gamma \rightarrow eH$  numerically with no  $H\gamma\gamma$  anomaly. When the  $H\gamma\gamma$  anomaly is known, this effect can be easily considered. The  $H\gamma\gamma$  anomaly often enhances the effective  $H\gamma\gamma$  coupling. In

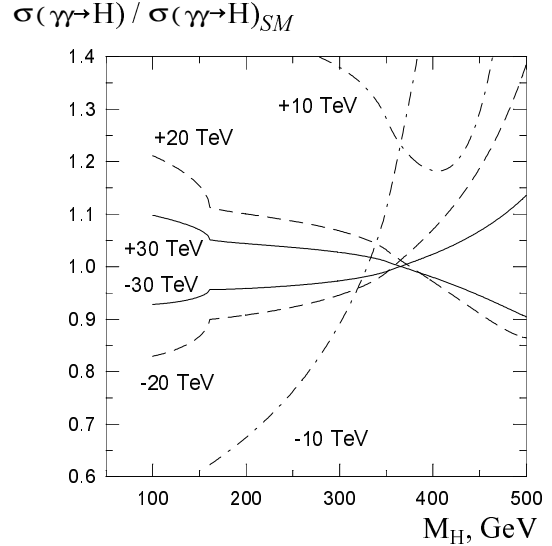


FIG. 7. The modification of the  $\gamma\gamma \rightarrow H$  cross section compared to its the  $SM$  value caused by anomalous interactions. The numbers denote  $\theta_\gamma\Lambda_\gamma$ .

this case, the effect of the  $ZH\gamma$  anomaly is also enhanced [see Eq. (14)] and the corresponding ultimate value of  $\Lambda_Z$  will be larger.

Figures 7 and 8 show cross sections of correspondent reactions for different  $\theta_i$  and  $\Lambda_i$ . Note that, in contrast to the  $MSM$  case, the observable effect in  $e\gamma \rightarrow eH$  process increases with growth of energy. This is due to the fact that the  $MSM$  components of effective couplings  $G_i$  decrease with  $Q^2$  growth in the  $SM$ , but their anomalous components are  $Q^2$  independent.

We estimated typical values  $\Lambda_i$  that can be observed in the reactions (1) at a luminosity integral of about  $100 \text{ fb}^{-1}$  for the wide interval of possible Higgs boson masses.

For the  $\gamma\gamma \rightarrow H$  process we used the following procedure. First, we took into account the branching ratio for the appropriate Higgs boson decay. After that, we estimated the number of main background events (for example,  $\gamma\gamma \rightarrow b\bar{b}$  for  $M_H < 140$  GeV,  $\gamma\gamma \rightarrow ZZ$  for  $M_H > 190$  GeV). Suppose then that the expected number of observed events calculated within the  $SM$  (with the above procedure) is  $N_0$ , while the number of events with considered effect is  $N_0 \pm \Delta N$ . We assume an effect to be observable if either  $\Delta N > 3\sqrt{N_0}$  (provided  $N_0 > 10$ ) or  $\Delta N > 10$  (provided  $N_0 < 10$ ).

For the  $e\gamma \rightarrow eH$  process we just compared the  $SM$  cross section to that calculated in presence of a  $HZ\gamma$  anomaly. The results for  $\Lambda$  are given in Table III. Results of an analysis of Ref. [4] correspond to  $\Lambda_\gamma \sim 10 \div 15$  TeV.

To obtain more realistic limitations a simulation is necessary with background analysis and some realistic detector imitation. Obviously, it reduces the ultimate values of  $\Lambda_i$  given in Table III. In particular, such a simula-

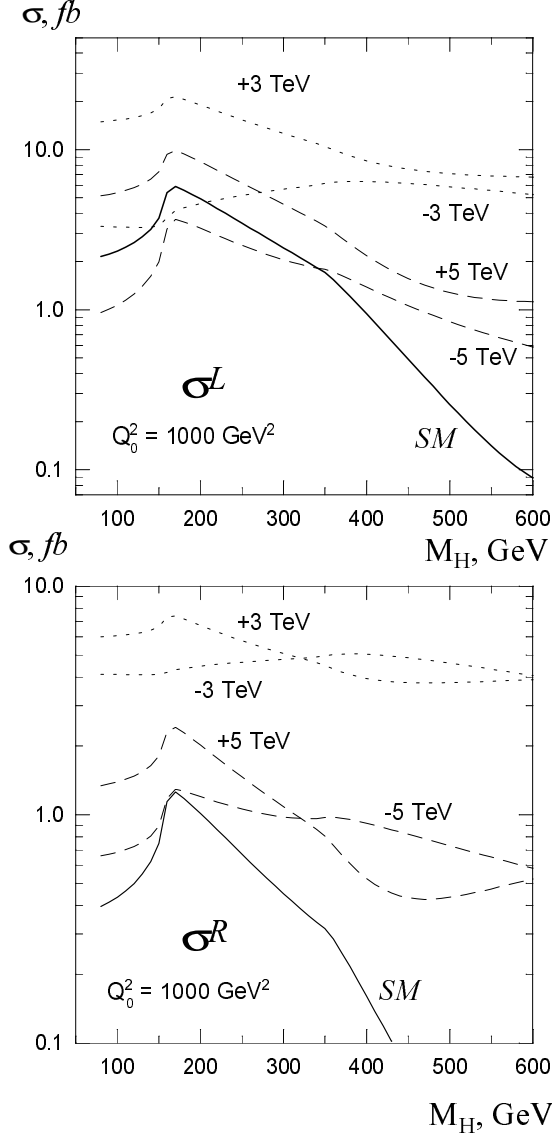


FIG. 8. The modification of the  $e\gamma \rightarrow eH$  cross sections compared to their the  $SM$  value caused by anomalous interactions. The numbers denote  $\theta_2\Lambda_Z$ . In the last case  $\Lambda_\gamma = \infty$  is assumed.

tion was performed in ref. [6] for the  $e\gamma \rightarrow eH$  reaction for  $M_H < 140$  GeV. In our terms the cross sections and background founded there correspond to  $\Lambda_Z = 8$  TeV, which should be compared to our estimate  $\Lambda_Z = 11$  TeV for  $M_H = 100$  GeV.

This comparison shows that our estimates give the correct order of the observability limits. We hope that the same will be true for the other values of the Higgs boson mass and consequently other decay modes.

Similar estimates for gluon fusion were obtained in Ref. [2]. The results mean in our notation that in future experiments at LHC one can hope to set limitations (for  $\mathcal{CP}$  even anomalous  $ggH$  interactions)  $\Lambda_g = 35$  TeV.

Recently several papers appeared aiming to establish

| $M_H$ , GeV | $\Lambda_\gamma$ , TeV | $\Lambda_Z$ , TeV |
|-------------|------------------------|-------------------|
| 100         | 60                     | 11                |
| 200         | 45                     | 9                 |
| 300         | 28                     | 8                 |
| 400         | 12                     | 7                 |
| 500         | 10                     | 8                 |
| 700         | 10                     | 10                |

TABLE III. Values of  $\Lambda_i$  for different  $M_H$  which can be probed at photon colliders.

bounds on anomalous  $\gamma\gamma H$  interactions from the existing LEP2 [30] or Tevatron [31] data. Different final states were used for this purpose ( $3\gamma$ ,  $\gamma\gamma + jj$ ,  $\gamma\gamma +$  missing energy), but all of them resulted in almost the same bound ( $\Lambda_\gamma \approx 1$  TeV). These limitations are weak in comparison with the values attainable at photon colliders (Table III).

#### IV. CONCLUSION

We considered major processes for the Higgs boson production at photon colliders and assessed the feasibility of the possible anomalous interactions study. We showed that photon colliders provide a spectacular field for the investigation of these phenomena. Future experiments at photon and hadron colliders can either reveal or completely rule out new heavy particles that can exist in the  $SM$  before a direct discovery of these heavy particles.

We derive constraints on a characteristic scale of the possible underlying theory that can be obtained from future experiments at  $\gamma\gamma$  or  $e\gamma$  colliders. The analysis of these scales in the framework of some specific models is the subject of further studies. The resultant values of  $\Lambda_i$  are rather large. This leads us to believe that the study of the Higgs boson physics at photon colliders will be an important step in probing Nature beyond the  $SM$ .

In this paper we analyzed processes that are most appropriate for the study of separate anomalies in the Effective Lagrangian. From this point of view the investigation of other processes should both support the results obtained from the discussed experiments and give information about new additional anomalies. For instance, the main potential of process  $\gamma\gamma \rightarrow HH$  concerns the study of anomalous Higgs boson self-interaction [32], the main potential of process  $e\gamma \rightarrow \nu WH$  is related to more complex anomalies such as  $WWH\gamma$ , etc. The study of processes in  $\gamma\gamma$  or  $e\gamma$  collisions has very high potential in these problems since small correction in anomaly is added here not to the relatively large tree effect but to the small one-loop contribution of the  $SM$ .

## ACKNOWLEDGEMENTS

We are thankful to V.A. Ilyin, M. Krawczyk and V.G. Serbo for discussions. This work was supported by grant RFBR No. 96-02-19079. .

---

\* E-mail: ginzburg@math.nsc.ru

- [1] I.F. Ginzburg, I.P. Ivanov, A. Schiller, hep-ph/9802364.
- [2] G.J. Gounaris, J. Layssac and F.M. Renard, Phys. Rev. **D58** (1998) 075006.
- [3] I.F. Ginzburg, Preprint 28(182) Inst. of Mathem., Novosibirsk (1990), Proc. 9th International Workshop on Photon – Photon Collisions, San Diego (1992) 474–501, World Sc. Singapore.
- [4] G.J. Gounaris, J. Layssac, F.M. Renard, Z. Phys. **C65** (1995) 505; G.J. Gounaris, F.M. Renard, Z. Phys. **C65** (1995) 513.
- [5] E. Gabrielli, V.A. Ilyin, B Mele, Phys. Rev. **D56** (1997) 5945.
- [6] E. Gabrielli, V.A. Ilyin and B. Mele, Proc. "Beyond the Standard Model V", (1997) 506.
- [7] A. Abbasabadi, D. Bowser-Chao, D.A. Dicus and W.A. Repko, Phys. Rev. **D52** (1995) 3919.
- [8] Particle Data Group. Eur. Phys J. **C3** (1998) 1.
- [9] I.F. Ginzburg, G.L. Kotkin, V.G. Serbo, V.I. Telnov. Pis'ma ZhETF **34** (1981) 514; Nucl.Instr.Methods (NIM) **205** (1983) 47. I.F.Ginzburg, G.L.Kotkin, S.L.Panfil, V.G.Serbo, V.I.Telnov. NIM **219** (1984) 5.
- [10] Zeroth-order Design Report for the NLC, SLAC Report 474 (1996); TESLA, SBLC Conceptual Design Report, DESY 97-048, ECFA-97-182 (1997); R.Brinkmann et. al., NIMR **A406** (1998) 13.
- [11] G.L. Kotkin, V.G. Serbo, Phys. Lett. **B413** (1997) 122.
- [12] D.L. Borden, D.A. Bauer, D.O. Caldwell, Phys. Rev. **D48** (1993) 4018; D.L. Borden, V.A. Khoze, W.J. Stirling, J.Ohnemus, Phys. Rev. **D50** (1994) 4499; O. Eboli, M. Gonzales-Garcia, F. Halzen, D. Zeppenfeld, Phys. Rev. **D48** (1993) 1430; T. Ohgaki, T. Takahashi, I. Watanabe, Phys. Rev. **D56** (1997) 1723.
- [13] I.F. Ginzburg, I.P. Ivanov, Phys. Lett. **408B** (1997) 325.
- [14] E. Boos et al, Phys. Lett. **B427** (1998) 189.
- [15] J.F. Gunion, L. Poggiolli and R. van Kooten, hep-ph/9703330 (1997).
- [16] G.V. Jikia, Nucl. Phys **B412** (1994) 57; G.V. Jikia, Yu.F. Pirogov, Phys. Lett. **B283** (1992) 135.
- [17] N.N. Achasov, Phys. Lett. **B222** (1989) 139.
- [18] O.J.P. Eboli, M.C. Gonzales-Garcia, Phys. Rev. **D49** (1994) 91.
- [19] U. Cotti, L.J. Diaz-Cruz and J.J. Toscano, Phys. Lett. **B404** (1997) 308
- [20] A.I Vainshtein, M.B. Voloshin, V.I. Zakharov, and M.A. Shifman, Sov. J. Nucl. Phys. **30** (1979) 711; L.B. Okun, Leptons and Quarks. North-Holland Physics Publishing, 1982, Amsterdam.
- [21] I.F. Ginzburg, V.G. Serbo, Phys. Lett. **103B** (1981) 68.
- [22] M. Spira, A. Djouadi, D. Graudenz, and P. M. Zerwas, Nucl. Phys. B **453**, 17 (1995); S. Dawson, R.P. Kauffman, Phys. Rev. **D47** (1993) 1264; V. Del Duca, R.C.R. Schmidt, Phys. Rev. **D49** (1994) 177; K. Melnikov, M. Spira, O. Yakovlev, Z. Phys. **C64** (1994) 491.
- [23] G.F. van Oldenborgh, *FF - a package to evaluate one-loop Feynman diagrams*, NIKHEP, H/90–15, September 1990; G.F. van Oldenborgh and J.A.M Vermaseren, Z. Phys. **C46** (1990) 425.
- [24] W.Buchmuller, D.Wyler. Nucl.Phys. **B268** (1986) 621.
- [25] C.I.C. Burges, H.I. Schnitzer. Nucl.Phys. **B228** (1983) 464; C.N. Leung, S.T. Love, S.Rao. Z.Phys. **C31** (1986) 433.
- [26] K. Hagiwara et al, Phys. Rev. **D 48** (1993) 2182; S. Dawson, S. Alam, R. Szalapski, Phys. Rev. **D57** (1998) 1577.
- [27] M.C. Gonzales-Garcia, hep-ph/9811389.
- [28] C. Arzt, M.B. Einhorn, J. Wudka, Nucl. Phys. **B433** (1995) 41.
- [29] I.F. Ginzburg, I.P. Ivanov, M. Krawczyk, in preparation.
- [30] O.J.P. Eboli, M.C. Gonzalez-Garcia, S.M. Lietti, S.F. Novaes, Phys.Lett., **B434** (1998) 340.
- [31] M.C. Gonzalez-Garcia, S.M. Lietti, S.F. Novaes, Phys. Rev. **D57** (1998) 7045; F. de Campos, M.C. Gonzalez-Garcia, S.F. Novaes, Phys. Rev. Lett. **79** (1997) 5210; F. de Campos, M.C. Gonzalez-Garcia, S.M. Lietti, S.F. Novaes, R. Rosenfeld, Phys. Lett. **B435** (1998) 407.
- [32] G. Jikia and A. Tkabladze, Phys. Lett. **B283** (1992) 135; V.A. Ilyin, A.E. Pukhov, Y. Kurihara, Y. Shimizu, T. Kaneko. Phys. Rev. **D 54** (1996) 6717.

## APPENDIX A: BOX ITEMS

Below we use additional notations:  $v_e = 1 - 4s_W^2$ ,  $t = -Q^2$ ,  $u = M_H^2 - s - t$  and  $\beta_{P\pm}$  (with quantities  $r_P$  from Eq. (10)) and use dilogarithm function  $Li_2(z)$ :

$$Li_2(z + i\varepsilon) = - \int_0^z \frac{dt}{t} \ln|1-t| + i\pi\theta(z-1) \ln z; \quad \beta_{P\pm} = \frac{1}{2} (1 \pm \sqrt{1-r_P}), \quad (P = Z, W).$$

The  $Z$  box or  $W$  box item below contains box diagrams and relevant  $s$  and  $u$ -channel triangle diagrams with  $Z$  or  $W$  boson circulating in loops.

### 1. Z Box items

In the numbering scheme of [7]  $Z$  box item is expressed in terms of scalar loop integrals

$$\begin{aligned} Z(s, u) = & -\frac{(v_e - \zeta_e)^2}{4c_W^4} \frac{s - M_Z^2}{2ts^2} \left\{ -\bar{D}_Z(1, 2, 3, 4) + \bar{C}_Z(1, 2, 3) + \bar{C}_Z(2, 3, 4) - \bar{C}_Z(1, 3, 4) \right. \\ & \left. + \left( \frac{t-s}{t+s} - 2M_Z^2 \frac{ts}{(M_H^2 - u)^2 (s - M_Z^2)} \right) \bar{C}_Z(1, 2, 4) + \frac{2ts}{(M_H^2 - u)(s - M_Z^2)} [B_Z(1, 4) - B_Z(2, 4)] \right\}. \end{aligned} \quad (A1)$$

We calculated these functions using explicit expressions from Ref. [7], rewritten for our process:

$$\begin{aligned} D_Z(1, 2, 3, 4) = & \ln\left(1 - \frac{s}{M_Z^2} - i\varepsilon\right) \left[ \ln\left(\frac{su}{m_Z^2 M_H^2} - i\varepsilon\right) + 2 \ln\left(1 - \frac{M_Z^2}{s}\right) + \ln\left(-\frac{M_Z^2}{s} + i\varepsilon\right) \right. \\ & \left. + \ln\left(1 - \frac{M_Z^2}{s} - \frac{M_Z^2}{u}\right) - \ln\left(\beta_{Z+} - \frac{M_Z^2}{s}\right) - \ln\left(\beta_{Z-} - \frac{M_Z^2}{s}\right) \right] \\ & + \ln\left(1 - \frac{u}{M_Z^2}\right) \left[ \ln\left(\frac{su}{m_Z^2 M_H^2} - i\varepsilon\right) + \ln\left(-\frac{M_Z^2}{u}\right) + 2 \ln\left(1 - \frac{M_Z^2}{u}\right) \right. \\ & \left. + \ln\left(1 - \frac{M_Z^2}{u} - \frac{M_Z^2}{s}\right) - \ln\left(\beta_{Z+} - \frac{M_Z^2}{u}\right) - \ln\left(\beta_{Z-} - \frac{M_Z^2}{u}\right) \right] - \frac{2\pi^2}{3} \\ & + 2Li_2\left(\frac{-\frac{M_Z^2}{s}}{1 - \frac{M_Z^2}{s}}\right) + Li_2\left(\frac{-\frac{M_Z^2}{s}}{1 - \frac{M_Z^2}{s} - \frac{M_Z^2}{u}}\right) - Li_2\left(\frac{-\frac{M_Z^2}{s}}{\beta_{Z+} - \frac{M_Z^2}{s}}\right) - Li_2\left(\frac{-\frac{M_Z^2}{s}}{\beta_{Z-} - \frac{M_Z^2}{s}}\right) \\ & - Li_2\left(\frac{1 - \frac{M_Z^2}{s}}{1 - \frac{M_Z^2}{s} - \frac{M_Z^2}{u}}\right) + Li_2\left(\frac{1 - \frac{M_Z^2}{s}}{\beta_{Z+} - \frac{M_Z^2}{s}} - i\varepsilon\right) + Li_2\left(\frac{1 - \frac{M_Z^2}{s}}{\beta_{Z-} - \frac{M_Z^2}{s}} + i\varepsilon\right) \\ & + 2Li_2\left(\frac{-\frac{M_Z^2}{u}}{1 - \frac{M_Z^2}{u}}\right) + Li_2\left(\frac{-\frac{M_Z^2}{u}}{1 - \frac{M_Z^2}{u} - \frac{M_Z^2}{s}}\right) - Li_2\left(\frac{-\frac{M_Z^2}{u}}{\beta_{Z+} - \frac{M_Z^2}{u}}\right) - Li_2\left(\frac{-\frac{M_Z^2}{u}}{\beta_{Z-} - \frac{M_Z^2}{u}}\right) \\ & - Li_2\left(\frac{1 - \frac{M_Z^2}{u}}{1 - \frac{M_Z^2}{u} - \frac{M_Z^2}{s}} - i\varepsilon\right) + Li_2\left(\frac{1 - \frac{M_Z^2}{u}}{\beta_{Z+} - \frac{M_Z^2}{u}} - i\varepsilon\right) + Li_2\left(\frac{1 - \frac{M_Z^2}{u}}{\beta_{Z-} - \frac{M_Z^2}{u}} + i\varepsilon\right); \end{aligned}$$

$$\bar{C}_Z(1, 2, 3) = -Li_2 \left( \frac{1}{1 - \frac{M_Z^2}{s}} - i\varepsilon \right) + \frac{1}{2} \ln^2 \left( 1 - \frac{s}{M_Z^2} - i\varepsilon \right);$$

$$\begin{aligned} \bar{C}_Z(1, 2, 4) &= Li_2 \left( \frac{\alpha_1 - 1}{\alpha_1} \right) + Li_2 \left( \frac{\alpha_2}{\alpha_2 - \beta_{Z-}} \right) - Li_2 \left( \frac{\alpha_2 - 1}{\alpha_2 - \beta_{Z-}} + i\varepsilon \right) \\ &+ Li_2 \left( \frac{\alpha_2}{\alpha_2 - \beta_{Z+}} \right) - Li_2 \left( \frac{\alpha_2 - 1}{\alpha_2 - \beta_{Z+}} - i\varepsilon \right) - Li_2 \left( \frac{\alpha_3}{\alpha_3 - 1} \right) - Li_2 \left( \frac{\alpha_3}{\alpha_3 - \frac{M_Z^2}{u}} \right) + Li_2 \left( \frac{\alpha_3 - 1}{\alpha_3 - \frac{M_Z^2}{u}} \right); \end{aligned}$$

$$\begin{aligned} \bar{C}_Z(1, 3, 4) &= Li_2 \left( \frac{\gamma - 1}{\gamma - 1 + \frac{M_Z^2}{s}} - i\varepsilon \right) - Li_2 \left( \frac{\gamma}{\gamma - 1 + \frac{M_Z^2}{s}} \right) + Li_2 \left( \frac{\gamma - 1}{\gamma} + i\varepsilon \right) \\ &+ Li_2 \left( \frac{\gamma}{\gamma - \beta_{Z-}} \right) - Li_2 \left( \frac{\gamma - 1}{\gamma - \beta_{Z-}} + i\varepsilon \right) + Li_2 \left( \frac{\gamma}{\gamma - \beta_{Z+}} \right) - Li_2 \left( \frac{\gamma - 1}{\gamma - \beta_{Z+}} - i\varepsilon \right) - \frac{\pi^2}{6}; \end{aligned}$$

$$\bar{C}_Z(2, 3, 4) = -Li_2 \left( \frac{1}{1 - \frac{M_Z^2}{u}} \right) + \frac{1}{2} \ln^2 \left( 1 - \frac{u}{M_Z^2} \right);$$

$$B_Z(1, 4) - B_Z(2, 4) = \sqrt{1 - r_Z} \ln \left( \frac{-\beta_{Z-}}{\beta_{Z+}} + i\varepsilon \right) - \left( 1 - \frac{M_Z^2}{u} \right) \ln \left( \frac{M_Z^2}{M_Z^2 - u} \right).$$

Here

$$\alpha_1 = 1 + \frac{M_H^2 M_Z^2 - M_H^4}{(M_H^2 - u)^2}, \quad \alpha_2 = \frac{M_Z^2}{M_H^2 - u}, \quad \alpha_3 = \frac{M_Z^2 M_H^2}{u(M_H^2 - u)}, \quad \gamma = \frac{M_Z^2}{M_H^2 - s}. \quad (\text{A2})$$

When  $u$  and  $s$  are switched in the above formulas,  $\bar{D}$  does not change at all, while  $\bar{C}_Z(1, 2, 3) \leftrightarrow \bar{C}_Z(2, 3, 4)$ ,  $\bar{C}_Z(1, 2, 4) \leftrightarrow \bar{C}_Z(1, 3, 4)$ .

## 2. W box items

The W box item can be written as

$$W(s, u) = (1 - \zeta_e) [A_1(t, s, u) + A_2(t, u, s)]; \quad (\text{A3})$$

$$\begin{aligned} A_1(t, s, u) &= \frac{s - M_W^2}{2ts^2} \left\{ (ts - tM_W^2 + M_W^2 M_H^2) D_W(1, 2, 3, 4) - \bar{C}_W(1, 2, 3) + \bar{C}_W(1, 2, 4) \right. \\ &\left. - \bar{C}_W(1, 3, 4) + \bar{C}_W(2, 3, 4) - \frac{2ts}{(M_H^2 - t)(s - M_W^2)} [B_W(1, 3) - B_W(1, 4)] \right\}. \end{aligned} \quad (\text{A4})$$

$$\begin{aligned} A_2(t, s, u) &= \frac{M_H^2 - M_W^2 - s}{2tu^2} \left\{ (M_W^2 M_H^2 - ts - 3M_W^2 t) D_W(1, 2, 3, 4) \right. \\ &\left. + \bar{C}_W(1, 2, 3) + \frac{u^2 - 2tu - t^2}{(M_H^2 - s)^2} \bar{C}_W(1, 2, 4) - \bar{C}_W(1, 3, 4) + \bar{C}_W(2, 3, 4) \right. \\ &\left. + \frac{2tu}{(M_H^2 - t)(M_H^2 - M_W^2 - s)} [B_W(1, 3) - B_W(1, 4)] + \frac{2tu}{(M_H^2 - s)(M_H^2 - M_W^2 - s)} [B_W(2, 4) - B_W(1, 4)] \right\}. \end{aligned} \quad (\text{A5})$$

In the decomposition of these functions in dilogarithms, etc., we used auxiliary notations

$$\begin{aligned}\alpha &= 1 - \frac{M_W^2}{s}, \quad \gamma_{\pm} = \frac{1}{2} \left( 1 \pm \sqrt{1 - \frac{r_W}{w}} \right), \\ \lambda_{\pm} &= \frac{1}{2} \left[ 1 + \frac{M_W^2(t - M_H^2)}{-ts} \pm \sqrt{\left( 1 + \frac{M_W^2(t - M_H^2)}{-ts} \right)^2 - \frac{4M_W^2}{t}} \right].\end{aligned}\tag{A6}$$

$$\begin{aligned}D_W(1, 2, 3, 4) &= -\frac{1}{ts(\lambda_+ - \lambda_-)} \left\{ \left[ -Li_2 \left( \frac{1 - \lambda_+}{\alpha - \lambda_+} \right) + Li_2 \left( \frac{-\lambda_+}{\alpha - \lambda_+} + i\varepsilon \right) \right. \right. \\ &\quad - Li_2 \left( \frac{1 - \lambda_+}{\gamma_+ - \lambda_+} \right) + Li_2 \left( \frac{-\lambda_+}{\gamma_+ - \lambda_+} \right) - Li_2 \left( \frac{1 - \lambda_+}{\gamma_- - \lambda_+} \right) \\ &\quad + Li_2 \left( \frac{-\lambda_+}{\gamma_- - \lambda_+} \right) + Li_2 \left( \frac{1 - \lambda_+}{\beta_{W+} - \lambda_+} \right) - Li_2 \left( \frac{-\lambda_+}{\beta_{W+} - \lambda_+} + i\varepsilon \right) \\ &\quad \left. \left. + Li_2 \left( \frac{1 - \lambda_+}{\beta_{W-} - \lambda_+} \right) - Li_2 \left( \frac{-\lambda_+}{\beta_{W-} - \lambda_+} - i\varepsilon \right) \right] \right. \\ &\quad \left. \left[ -Li_2 \left( \frac{1 - \lambda_-}{\alpha - \lambda_-} - i\varepsilon \right) + Li_2 \left( \frac{-\lambda_-}{\alpha - \lambda_-} \right) - Li_2 \left( \frac{1 - \lambda_-}{\gamma_+ - \lambda_-} \right) + Li_2 \left( \frac{-\lambda_-}{\gamma_+ - \lambda_-} \right) \right. \right. \\ &\quad - Li_2 \left( \frac{1 - \lambda_-}{\gamma_- - \lambda_-} + i\varepsilon \right) + Li_2 \left( \frac{-\lambda_-}{\gamma_- - \lambda_-} + i\varepsilon \right) + Li_2 \left( \frac{1 - \lambda_-}{\beta_{W+} - \lambda_-} - i\varepsilon \right) \\ &\quad \left. \left. - Li_2 \left( \frac{-\lambda_-}{\beta_{W+} - \lambda_-} \right) + Li_2 \left( \frac{1 - \lambda_-}{\beta_{W-} - \lambda_-} + i\varepsilon \right) - Li_2 \left( \frac{-\lambda_-}{\beta_{W-} - \lambda_-} \right) \right] \right\} \\ \bar{C}_W(1, 2, 3) &= -\frac{\pi^2}{6} + Li_2 \left( 1 - \frac{t}{M_W^2} + i\varepsilon \right) + Li_2 \left( \frac{M_W^2}{M_W^2 - t\gamma_+} \right) \\ &\quad - Li_2 \left( \frac{M_W^2 - t}{M_W^2 - t\gamma_+} \right) + Li_2 \left( \frac{M_W^2}{M_W^2 - t\gamma_-} + i\varepsilon \right) - Li_2 \left( \frac{M_W^2 - t}{M_W^2 - t\gamma_-} + i\varepsilon \right), \\ \bar{C}_W(1, 3, 4) &= Li_2 \left( \frac{1}{\gamma_+} \right) + Li_2 \left( \frac{1}{\gamma_-} \right) - Li_2 \left( \frac{1}{\beta_{W+}} - i\varepsilon \right) - Li_2 \left( \frac{1}{\beta_{W-}} + i\varepsilon \right), \\ \bar{C}_W(2, 3, 4) &= -Li_2 \left( \frac{s}{M_W^2} + i\varepsilon \right)\end{aligned}$$

and  $\bar{C}_W(1, 2, 4)$  can be obtained from  $\bar{C}_Z(1, 3, 4)$  by replacing  $m_Z \rightarrow m_W$ .

$$\begin{aligned}B_W(1, 3) - B_W(1, 4) &= \sqrt{1 + \frac{r_W}{w}} \ln \left( -\frac{\gamma_-}{\gamma_+} \right) - \sqrt{1 - r_W} \ln \left( -\frac{\beta_{W-}}{\beta_{W+}} + i\varepsilon \right) \\ B_W(2, 4) - B_W(1, 4) &= \left( 1 - \frac{M_W^2}{s} \right) \ln \left( \frac{M_W^2}{M_W^2 - s} + i\varepsilon \right) - \sqrt{1 - r_W} \ln \left( -\frac{\beta_{W-}}{\beta_{W+}} + i\varepsilon \right).\end{aligned}$$

### 3. The used functions and those from the FF package

These used functions can be evaluated numerically by means of FF package [23]. The full sets of arguments for these functions are:

$$\begin{aligned}\bar{D}_Z(1, 2, 3, 4) &= (su + M_Z^2 t - M_Z^2 M_H^2) D_0(M_Z^2, m_e^2, m_e^2, M_Z^2, 0, 0, 0, M_H^2, s, u) \\ &+ \left[ \ln\left(1 - \frac{s}{M_Z^2} - i\varepsilon\right) + \ln\left(1 - \frac{u}{M_Z^2}\right) \right] \ln\left(\frac{m_e^2}{M_Z^2}\right);\end{aligned}$$

$$\bar{C}_Z(1, 2, 3) = sC_0(m_e^2, m_e^2, M_Z^2, 0, 0, s) + \ln\left(1 - \frac{s}{M_Z^2} - i\varepsilon\right) \ln\left(\frac{m_e^2}{M_Z^2}\right);$$

$$\bar{C}_Z(1, 2, 4) = (M_H^2 - u)C_0(m_e^2, M_Z^2, M_Z^2, 0, M_H^2, u);$$

$$\bar{C}_Z(1, 3, 4) = (M_H^2 - s)C_0(m_e^2, M_Z^2, M_Z^2, 0, M_H^2, s);$$

$$\bar{C}_Z(2, 3, 4) = uC_0(m_e^2, m_e^2, M_Z^2, 0, 0, u) + \ln\left(1 - \frac{u}{M_Z^2}\right) \ln\left(\frac{m_e^2}{M_Z^2}\right);$$

$$B_Z(1, 4) - B_Z(2, 4) = B_0(M_Z^2, M_Z^2, M_H^2) - B_0(m_e^2, M_Z^2, u).$$

$$D_W(1, 2, 3, 4) = D_0(M_W^2, 0, M_W^2, M_W^2, 0, 0, 0, M_H^2, t, s);$$

$$\bar{C}_W(1, 2, 3) = tC_0(0, M_W^2, M_W^2, 0, t, 0); \quad \bar{C}_W(1, 2, 4) = (M_H^2 - s)C_0(0, M_W^2, M_W^2, 0, M_H^2, s);$$

$$\bar{C}_W(1, 3, 4) = (M_H^2 - t)C_0(M_W^2, M_W^2, M_W^2, t, 0, M_H^2); \quad \bar{C}_W(2, 3, 4) = sC_0(0, M_W^2, M_W^2, 0, 0, s);$$

$$B_W(1, 3) - B_W(1, 4) = B_0(M_W^2, M_W^2, t) - B_0(M_W^2, M_W^2, M_H^2) :$$

$$B_W(2, 4) - B_W(1, 3) = B_0(0, M_W^2, s) - B_0(M_W^2, M_W^2, M_H^2).$$

Together with different normalization, our functions differ from those used in FF package by the absence of large logarithms  $\ln(m_e^2/M_Z^2)$  (which disappear in the final result in both approaches).